C.P. No. 515
(21,032)
A.R.C. Technical Report

C.P. No. 515
(21,032)
A.R.C. Technical Report

MINISTRY OF AVIATION

AERONAUTICAL RESEARCH COUNCIL

CURRENT PAPERS

Static Tests on a Conical Centrebody Supersonic Air Intake with an Auxiliary Air Inlet Slot

By

M. COX

LONDON: HER MAJESTY'S STATIONERY OFFICE

1960

PRICE 3s 6d NET

U.D.C. No. 533.697.22

C.P. No. 515

Memorandum No. M.323
February, 1959

NATIONAL GAS TURBINE ESTABLISHMENT

Static tests on a conical centrebody supersonic air intake with an auxiliary air inlet slot

- by -

M. Cox

SUMMARY

Tests on a sharp-lipped supersonic intake have shown that at zero flight speed the total pressure recovery is improved from 0.78 to 0.97 by opening an annular auxiliary air inlet, at a compressor entry Mach number of 0.5. At the same time the ratio of peak to mean velocity at the compressor entry is reduced from 1.3 to 1.1.

A simple method is given of calculating changes in pressure recovery with intake flow rate and bleed slot opening, which should be applicable to other intake and auxiliary inlet configurations.

Note:-

This paper describes experiments limited to one particular intake configuration. It does not seek to formulate a precise theory of behaviour confirmed in detail by experiments, but rather to illustrate how nearly overall characteristics can be described by a much-simplified model.

CONTENTS

TABLES

APPENDICES

ILLUSTRATIONS

1.0 Introduction

Aircraft engine intakes for supersonic flight speeds have sharp-edged inlet cowls, and in consequence considerable losses in total pressure of the entering air occur when the aircraft is moving at low forward speeds, particularly under take-off conditions. One way of reducing this loss is to open auxiliary air inlets in the side of the intake so that the inlet is partially bypassed at low forward speeds. With a particular type of engine in mind, which would operate at flight speeds up to Mach 4, it was desired to know what intake pressure recoveries could be assumed at take-off conditions.

2.0 Test apparatus

The model intake is shown in Figure 1. It has a single cone centrebody of 30° semi-angle positioned for shock on lip operation at $M = 4$. The forward end of the cowl is arranged to slide forward to provide an annular slot which forms the auxiliary air inlet. The internal surfaces of the cowl and centrebody are provided with a number of static pressure measuring holes and at the diffuser outlet in the plane of the compressor entry there are three total head combs disposed circumferentially at 120°. The combs are mounted on a rotatable section so that the whole outlet flow area can be explored. The leading dimensions of the intake passages are shown in Figure 2, together with the blockage of the annulus caused by the three support webs which remain fixed with respect to the centrebody.

The intake was bolted to a suction main in which the airflow was measured by means of an orifice plate installed in accordance with the British Standard Specifications.

3.0 Test results

3.1 Evaluation of pressure recovery

The pressure recovery, η, is the ratio of the mean total head of the flow at the measuring plane (compressor entry) to the ambient pressure. The mean total pressure could be evaluated in two ways. At each operating condition readings were taken on the total head combs at a number of radial positions; from these readings the area weighted mean total pressure was evaluated, and hence η. The second method was to measure the mass flow through the intake and the static pressure at the measuring plane. From these measurements the mean Mach number at the measuring plane was calculated. The mean total pressure was then evaluated as the sum of the static pressure and the dynamic head corresponding to the mean Mach number. In only one or two instances did the pressure recoveries evaluated by the two methods differ by more than 0.003, and, in what follows, results evaluated by the second method are quoted as these appeared to be slightly more consistent than the total pressure traverse measurements, possibly owing to the relatively long period of time required to take the latter readings.

3.2 Pressure recovery characteristics

In Figure 3 are shown the pressure recovery characteristics of the intake without and with the auxiliary air inlet. The uppermost curve was obtained after the original configuration had been modified by machining a radius on the slot which allowed the bleed air to enter the duct more easily (see Figure 2). It is clear from these curves that quite a modest forward movement of the cowl, equal to about 0.28 of the cowl inlet radius, is sufficient to improve the pressure recovery from 0.79 to 0.972 at the representative compressor entry Mach number of 0.5.

An alternative method of presentation is shown in Figure 4, in which the pressure recovery is related to the mass flow through the intake. The latter is plotted as a ratio of the actual flow to the flow which theoretically could pass the narrowest cross-section of the intake duct assuming ambient total pressure and sonic velocity at this point. With the slot shut, the maximum value of this flow ratio is about 0.787, and the shape of the curve is similar to that observed in other tests[2] on sharp-lipped intakes.

3.3 Velocity distribution

In Figure 5 are shown the measured velocity profiles at the compressor entry plane for two cases, one with the bleed slot shut, the other with it one inch open. It is seen that the bleed also very considerably improves the velocity distribution and reduces the peak velocity from 1.31 to 1.095 of the mean velocity.

4.0 Analysis of intake pressure recovery with slot shut

The losses in total pressure in the intake duct and the restriction of the maximum flow rate to about 80 per cent of its theoretical value are due to the occurrence of a vena contracta in the flow as it enters the intake. The flow conditions will now be discussed in terms of a simplified duct, such as that shown in Figure 6. The flow enters to form a vena contracta at station 2; it then mixes with the "dead" air to fill the duct at station 3. Diffusion then occurs up to the measuring section at station 4. As the Mach number is increased at station 4, the flow system passes through three regimes. Initially the flow is subsonic throughout, and P_{s_2}', the static pressure in the dead air space surrounding the vena contracta is equal to the static pressure P_{s_2} of the flow at this point. At some higher M_4 value, the flow in the vena contracta becomes sonic and thereafter P_{s_2}' is lower than P_{s_2}. At a still higher value of M_4, M_3 reaches a limiting value, and the intake is choked. Thereafter shocks occur in the diffuser which allow the lower pressures and higher Mach numbers to be attained at station 4 until eventually M_4 reaches 1 when the back pressure is reduced to a sufficiently low value.

These flow conditions have been analysed in Appendix II on the assumption that the flow is one-dimensional. If the state of the flow at station 3 is known, the contraction coefficient C at the vena contracta and the static pressure P_{s_2}' can be calculated by applying the condition of constant momentum between stations 2 and 3. Since the foregoing measurements have been made at station 4, an assumption has to be made as to the energy losses in the diffuser, and it has been assumed that the isentropic efficiency of this component is 0.9. The resulting change of contraction coefficient with pressure ratio is shown in Figure 7. The course of the points agrees very well with the theoretical curves of Jobson[1]; the incompressible contraction coefficient ($P_{s_2}/P_{t_1} = 1$) is about 0.55 and, therefore, Jobson's treatment, which is incomplete when C_i exceeds 0.7, may be taken to apply.

Using the one-dimensional theory with $C_i = 0.536$ and 0.90 diffuser efficiency, the observed values have been compared with the theoretical pressure recovery values on Figure 8. The practically constant relation of observed total pressure loss to a function of the measuring section Mach number suggests the method of presentation of results shown on Figure 9.

The same theory may also be used to estimate the changes in static pressure in the diffuser. These are shown in Figure 10 on which the measured wall static pressures are also plotted. The differences between the observed and calculated values are an indication of shortcomings of the assumptions made in respect of the completeness of mixing and one-dimensional flow pattern in the duct.

5.0 Analysis of intake pressure recovery with slot open

When the cowl is moved forward an annular slot is provided for ambient air to be drawn into the intake duct upstream of the compressor entry. If the flow conditions are known in the intake duct just upstream of the bleed slot, the effective total pressure of the entering bleed air may be estimated from the resultant total pressure of the flow at the compressor entry station. The method is described in Appendix III. In order to carry out the calculation, it is necessary also to know the proportion of the total flow which enters through the intake proper. In the experiments this was estimated by blanking off the slot and determining the relation between the airflow rate and the readings of static pressure on the inner surface of the cowl. Because the forward movement of the cowl changes the intake entry area, this calibration was made for each of the cowl positions (see Figure 12). When air was entering the bleed slot, the flow through the intake inlet was estimated from the cowl internal static pressure measurements.

The results of this analysis are shown in Table II. The conclusion is that the effective total pressure of the bleed air is about 0.99 of the ambient pressure. It is also of interest to compare the estimated static pressure in the flow through the bleed slot with the static pressure in the intake duct at the point where the two flows first meet. It is seen (Table II) that the two pressures are very similar. From this it follows that a suitable method for estimating the flow through the bleed slot is to assume the equality of the static pressures of the two flows at this point. By making a further assumption that there is a 15 per cent loss of dynamic head in the bleed flow, the resultant pressure recovery of the intake may be estimated. This estimation is laid out in Table III, and a comparison with observed pressure recoveries shows differences less than 0.003 in each case.

6.0 Discussion

It must be said that the auxiliary bleed arrangement on the present model is an almost ideal configuration. The entry is a well-rounded annulus obstructed only by three narrow struts and admits the air into the duct at its maximum cross-section. One may compare the recovery obtained in the present case with the cowl moved one inch forward (equivalent to 0.28 of the inlet radius) when the pressure recovery was 0.972 (2.8 per cent loss) with the 0.9 recovery (10 per cent loss) of a similar arrangement described elsewhere[3]. In the latter case the bleed slot was positioned very close to the intake throat, and also had a rather poorly faired entry. The importance of the shape of the bleed slot is illustrated in the present tests by the fact that the loss in total pressure at the measuring plane was approximately halved by introducing the radius at the downstream edge of the bleed slot.

The measure of agreement between the actual pressure recoveries with bleed flow and those calculated by the simple theory presented is an indication of the ideal nature of the auxiliary inlet. However, it is suggested that the method is suitable for studying problems of this sort and could be applied to other configurations by introducing an amended loss factor for the bleed air.

7.0 Conclusions

Tests on a model conical centrebody supersonic intake have shown that the pressure recovery of the intake when fitted with a well-designed auxiliary inlet can be 0.97 under static conditions. The velocity profile of the flow at the compressor entry plane is much improved by the auxiliary inlet, and in the present instance the ratio of maximum to mean velocity was decreased from 1.3 to 1.1 when the auxiliary inlet was opened.

The variations of pressure recovery with flow rate of a sharp-lipped inlet are adequately described by a simple one-dimensional theory using the method of Jobson for determining the variation of inlet discharge coefficient with flow rate.

It is shown that the auxiliary inlet tested is of an ideal type in that there is a very small loss of energy in introducing the air through the auxiliary inlet. A simple method is, therefore, adequate for determining the performance of the intake with auxiliary inlet.

REFERENCES

No.	Author(s)	Title, etc.
1	D. A. Jobson	On the flow of a compressible fluid through orifices. Proc. I.Mech.E. Vol. 169, 1955, p. 767.
2	A. H. Robinson	Pressure recovery of a model square-section, sharp-lip, internal compression intake at zero flight speed. A.R.C. 20,234 April 1958.
3	E. M. Cortright	Preliminary investigation of a translating cowl technique for improving take-off performance of a sharp lip supersonic diffuser. N.A.C.A. RM E51I24, November 1951.

TABLE I

Estimation of intake inlet contraction coefficient

M_4 (observed)	0.159	0.280	0.362	0.502
$\frac{P_{t4}}{P_{t1}}$ (observed)	0.9733	0.926	0.8835	0.788
M_3	0.214	0.385	0.513	0.692
$\frac{P_{t3}}{P_{t1}}$	0.9765	0.935	0.899	0.866
C	0.559	0.608	0.683	0.787
$\frac{P_{s2'}}{P_{t1}}$ (calculated)	0.896	0.685	0.493	0.245
$\frac{P_{s2'}}{P_{t1}}$ (observed)	0.899	0.687	0.484	0.197
f	0.116	0.127	0.129	0.189
C_i	0.532	0.536	0.539	0.551

TABLE II

Estimation of bleed flow pressure recovery and bleed slot static pressure

Cowl position x inch	0.5	1.0	1.5	2.0
$\frac{W_4\sqrt{T}}{A_4\ P_{t1}}$ (observed)	0.279	0.287	0.290	0.2923
P_{t4}/P_{t1} (observed)	0.9405	0.9718	0.9815	0.9876
$\frac{W_1\ \sqrt{T}}{A_4\ \ P_{t1}}$	0.205	0.1657	0.1375	0.1056
$\frac{P_{S4}'}{P_{t1}}$ (observed)	0.851	0.9115	0.941	0.963
$\frac{W_5\ \sqrt{T}}{A_4\ \ P_{t1}}$ (by difference)	0.074	0.1213	0.1525	0.1867
P_{t5}'/P_{t1} (calculated)	0.984	0.998	0.991	0.991
Bleed slot area A_5	5.95	12.14	18.8	26.0
$\frac{W_5\ \sqrt{T}}{A_5\ \ P_{t1}}$	0.3003	0.2412	0.1960	0.1734
$\frac{P_{S5}}{P_{t1}}\ \left(\text{cp}\ \frac{P_{S4}'}{P_{t1}}\right)$	0.838	0.903	0.939	0.953
$\frac{P_{t1}\ -\ P_{t5}'}{P_{t1}\ -\ P_{S5}}$	0.099	0.021	0.148	0.192

These results refer to tests with the radius on the downstream corner of the bleed slot.

TABLE III

Estimation of pressure recovery with bleed slot open from performance with no bleed

		0.5	1.0	1.5	2.0
	Forward movement of cowl x - inches	0.5	1.0	1.5	2.0
Observed values with slot blanked	M_4	0.514	0.502	0.502	0.511
	η	0.8515	0.8865	0.8925	0.8615
	$\frac{(1-\eta)}{M_4^2} \cdot \frac{P_{t4}}{P_{s4}}$ (X)	0.672	0.535	0.506	0.634
For A_4' = A_4 = 24.15 in²	M_4' (Guessed value)	0.35	0.26	0.21	0.16
	$P_{t'4}/P_{t1}$ (Calculated from X)	0.9242	0.9655	0.9784	0.9850
Correct to actual area A_4'	A_4' sq.in.	24.15	23.7	22.6	21.5
	M_4'	0.35	0.2653	0.225	0.182
	$\frac{P_{s4'}}{P_{t4'}}$	0.9188	0.9523	0.9654	0.9767
	$\frac{P_{s'4}}{P_{t1}}$	0.850	0.920	0.944	0.9615
Calculated pressure recovery	$\frac{W_1\sqrt{T}}{P_{t1}}$ (From M_4')	5.07	3.99	3.31	2.57
	$\frac{W_5\sqrt{T}}{P_{t1}}$ $\left(\text{From } \frac{P_{s5}}{P_{t1}} = \frac{P_{s4'}}{P_{t1}}\right)$	1.718	2.688	3.53	4.08
	$\frac{W_4\sqrt{T}}{P_{t1}} = (W_1 + W_5)$	6.788	6.678	6.84	6.65
	$\frac{P_{t5'}}{P_{t1}} \left(= 1 - 0.15\left(1 - \frac{P_{s5}}{P_{t1}}\right)\right)$	0.9775	0.9880	0.9916	0.9942
	$\frac{W_1 \; P_{t4'} + W_5 \; P_{t5'}}{W_4} = \frac{P_{t4}}{P_{t1}}$	0.9382	0.9738	0.9854	0.9910
	M_4 (From W_4 and P_{t4})	0.509	0.4725	0.480	0.459
	$\frac{1-\eta}{M_4^2} \cdot \frac{P_{t4}}{P_{s4}}$ (Y)	0.285	0.137	0.0743	0.0494
Comparison with experiment	M_4 (Observed value)	0.501	0.498	0.501	0.500
	$\frac{P_{t4}}{P_{t1}}$ (Observed value)	0.9405	0.9718	0.9815	0.9876
	$\frac{P_{t4}}{P_{t1}}$ (Calculated from Y)	0.9396	0.9714	0.9843	0.9896

APPENDIX I

List of symbols

A	Area
$\frac{A}{A_*}$	$\frac{\text{Cross section area}}{\text{Area at which } M = 1} = \frac{1}{M}\left[\frac{2}{\gamma + 1}\left(1 + \frac{\gamma - 1}{2} M^2\right)\right]^{\frac{\gamma+1}{2\gamma-2}}$
C	Contraction coefficient
C_i	C when $M \rightarrow 0$
$\bar{D}$	Stream thrust function $= \frac{A}{A_*} \cdot \frac{P_s}{P_t} (1 + \gamma M^2)$
F	Jobson's "Force defect"
f	Force defect coefficient
M	Mach number
P_t	Total pressure
P_s	Static pressure
T	Total temperature
W	Mass flow rate
x	Forward movement of cowl from slot closed position
η	Intake total pressure recovery
γ	Ratio of specific heats
ρ	Density

APPENDIX II

One-dimensional analysis of intake diffuser flow conditions

Referring to Figure 6, it is assumed that the intake passage area is constant from the inlet plane to the plane 3 where it is assumed that mixing is complete.

For constant stream thrust from plane 2 to plane 3

$$P_{S2'}\ (A_2 - C.A_2) + A_2.C\ (P_{S2} + P_{S2}\ \gamma M_2^2) = A_3 P_{S3}\ (1 + \gamma M_3^2) \qquad \ldots \quad (1)$$

where C is the contraction coefficient at the vena contracta

$$\frac{P_{S2'}}{P_{t1}}(1 - C) + C\,\frac{P_{S2}}{P_{t1}}(1 + \gamma M_2^2) = \frac{P_{S3}}{P_{t1}}(1 + \gamma M_3^2)$$

If it is assumed that the total pressure is constant up to the vena contracta, then from considerations of continuity

$$\frac{C.A_2\ P_{t1}}{(A/A_*)_2} = \frac{A_3\ P_{t3}}{(A/A_*)_3}$$

$$\frac{P_{t3}}{P_{t1}} = C\,\frac{(A/A_*)_3}{(A/A_*)_2} \qquad \ldots \quad \ldots \quad (2)$$

$$\frac{P_{S2'}}{P_{t1}}(1 - C) + C\left[\frac{P_S}{P_t}(1 + \gamma M^2)\right]_2 = C\,\frac{(A/A_*)_3}{(A/A_*)_2}\left[\frac{P_S}{P_t}(1 + \gamma M^2)\right]_3$$

$$\frac{P_{S2'}}{P_{t1}} \cdot \left(\frac{A}{A_*}\right)_2 \cdot \frac{1 - C}{C} + \left[\frac{A}{A_*} \cdot \frac{P_S}{P_t}(1 + \gamma M^2)\right]_2 = \left[\frac{A}{A_*} \cdot \frac{P_S}{P_t}(1 + \gamma M^2)\right]_3$$

Putting $\overline{D} = \frac{A}{A_*}\ \frac{P_S}{P_t}(1 + \gamma M^2)$, a function of M,

$$\frac{P_{S2'}}{P_{t1}}\left[\left(\frac{A}{A_*}\right)_3 \cdot \frac{P_{t1}}{P_{t3}} - \left(\frac{A}{A_*}\right)_2\right] + \overline{D}_2 = \overline{D}_3 \qquad \ldots \quad \ldots \quad (3)$$

Let us suppose that we know the Mach number and pressure recovery P_{t3}/P_{t1} at station 3. Two conditions are possible at the vena contracta. Either $M_2 < 1$, in which case $P_{S2'} = P_{S2}$, or $M_2 = 1$ in which case $(A/A_*)_2 = 1$ and $\overline{D}_2$ is known. By assuming values for M_2 and substituting in Equation (3) with $P_{S2'} = P_{S2}$, either a value of M_2 can be found which satisfies the equation, or it becomes clear that the flow in the vena contracta is sonic, and in either case C may be evaluated from Equation (2).

The conditions at station 3 are estimated from the observed conditions at station 4 by assuming a diffuser efficiency η_d defined by

$$\frac{P_{t4}}{P_{s3}} = \left[\frac{T_{s3} + \eta_d(T_{t3} - T_{s3})}{T_{s3}}\right]^{\frac{\gamma}{\gamma-1}}$$

The total pressure ratio along the diffuser is then

$$\frac{P_{t4}}{P_{t3}} = \frac{\left(1 + \eta_d \frac{\gamma - 1}{2} M_3{}^2\right)^{\frac{\gamma}{\gamma-1}}}{\left(1 + \frac{\gamma - 1}{2} M_3{}^2\right)^{\frac{\gamma}{\gamma-1}}}$$

$$= \frac{(P_t/P_s)_{M = \sqrt{\eta_d}\, M_3}}{(P_t/P_s)_{M = M_3}} \qquad \ldots \quad \ldots \quad (4)$$

It has been assumed that $\eta_d = 0.9$, so that it is then possible to determine a value of M_3 which satisfies both Equation (4) and the requirement of continuity between stations 3 and 4.

Application of Jobson's method

Following the method of Jobson, the equation of motion of the flow up to the vena contracta may be written

$$P_{t1}\, A_2 + F = P_{s2'}\, A_2\, (1 - C) + P_{s2}\, A_2\, C\, (1 + \gamma M^2) \qquad \ldots \quad \ldots \quad (5)$$

The term F, called the force defect, is introduced to allow for forces on surfaces upstream of the entry area, which are due to the negative pressure gradient in the flow as it accelerates before entering the inlet. It is assumed that

$$F = f \cdot \frac{W^2}{\rho_{t1}\, A_2}$$

where f is a constant for a particular orifice or inlet. With Equation (1), Equation (5) becomes

$$P_{t1}\, A_2 + f\, \frac{W^2}{\rho_{t1}\, A_2} = P_{s3}\, A_3\, (1 + \gamma M_3{}^2)$$

$$W = \rho_{s3}\, A_3\, V_3$$

$$W^2 = \rho_{s3}{}^2\, A_3{}^2\, M_3{}^2\, \frac{\gamma P_{s3}}{\rho_{s3}}$$

$$P_{t1}\, A_2 + f \cdot \gamma P_{s3} \cdot \frac{\rho_{s3}}{\rho_{t1}} \cdot A_3\, M_3{}^2 = P_{s3}\, A_3\, (1 + \gamma M_3{}^2)$$

whence

$$f = \frac{\rho_{t3}}{\rho_{s3}} \frac{P_{t1}}{P_{t3}} \left[1 - \frac{1}{\gamma M_3^2} \left(\frac{P_{t3}/P_{s3}}{P_{t3}/P_{t1}} - 1 \right) \right] \quad \ldots \quad (6)$$

$$\frac{P_{t3}}{P_{t1}} = \left[\frac{2\, P_t/P_s}{1 + \gamma M^2 + \left[(1 + \gamma M^2)^2 - 4f\gamma M^2 \cdot \frac{P_t}{P_s} \cdot \frac{\rho_s}{\rho_t} \right]^{\frac{1}{2}}} \right]_3 \quad \ldots \quad (7)$$

In Table 1, values of f calculated from the observed pressure recoveries are shown, together with the equivalent incompressible discharge coefficients C_i, given by

$$f = \frac{1}{C_i} - \frac{1}{2C_i^2}$$

So far, no restriction has been put on the value of $P_{s2'}$, and as may be inferred from Equation (3), M_3 will reach 1 if $P_{s2'}$ becomes zero. Observation shows however that $P_{s2'}$ has a positive value even when the intake is choked (i.e. when W/W_* has reached a constant maximum value). Referring to Figure 6, let it be supposed that, when $M_2 = 1$, the air continues to expand supersonically to some plane 2' at which the static pressure is $P_{s2'}$. The limit is then reached when $A_2' = A_2 = A_3$, and for constant momemtum between planes 2 and 2', with $M_2' > 1$, we have

$$\frac{P_{s2'}}{P_{t1}} (1 - C) + C \frac{P_{s2}}{P_{t1}} (1 + \gamma M_2^2) = \frac{P_{s2'}}{P_{t1}} (1 + \gamma M_2'^2)$$

and $$P_{t2'} \left(\frac{A_*}{A} \right)_{2'} = P_{t1} \times C$$

whence $$1 - C = \frac{\bar{D}_2' - \bar{D}_2}{(P_s/P_t \cdot A/A_*)_{2'}} \quad \ldots \quad (8)$$

The limit line defined by this equation is shown on Figure 7. The value of M_3 at the limit is given by

$$\bar{D}_3 = \bar{D}_{2'}$$

which merely expresses the conservation of stream thrust in a normal shock.

From the results of Table I a mean value of 0.126 has been chosen for f, and using Equation (7), the theoretical curve shown on Figure 8 has been drawn. Again Equation (8) has been used to define the limiting value of $P_{s2'}$, so that at high values of M_4, the theoretical curve breaks away as shown. Once having found the limiting values of M_3 and P_{t3}, the relationship between M_4 and P_{t4} follows from considerations of continuity between stations 3 and 4.

A worked example

Suppose that we have an intake similar to that described but with $A_4 = 1.5\ A_3$ and for which $P_{t4}/P_{t1} = 0.911$ when $M_4 = 0.36$. It is required to find the limiting value of W/W_*.

In order to determine M_3 at the given condition, we have Equation (4) above for P_{t4}/P_{t3} and the continuity equation

$$\left(\frac{A}{A_*}\right)_4 \times \frac{P_{t3}}{A_4} = \left(\frac{A}{A_*}\right)_3 \times \frac{P_{t4}}{A_3}$$

One or two trial calculations with guessed values of M_3 show that the two requirements are satisfied by $M_3 = 0.5$. Thus,

$$M_3 = 0.5, \quad \left(\frac{P_t}{P_s}\right)_3 = 1.1862, \quad \left(\frac{A}{A_*}\right)_3 = 1.3398$$

$$\sqrt{\eta_d}\ M_3 = \sqrt{0.9} \times 0.5 = 0.4744, \quad \frac{P_t}{P_s} = 1.1666$$

Therefore
$$\frac{P_{t4}}{P_{t3}} = \frac{1.1666}{1.1862} = 0.9835$$

$$\left(\frac{A}{A_*}\right)_4 = 1.3398 \times 0.9835 \times 1.5$$
$$= 1.7363$$

whence $M_4 = 0.36$

$$\frac{P_{t3}}{P_{t1}} = \frac{P_{t3}}{P_{t4}} \times \frac{P_{t4}}{P_{t1}}$$
$$= \frac{0.911}{0.9835}$$
$$= 0.926$$

Using Equation (6) we now find the value of f to be 0.2407 and the value of C_i is

$$C_i = \frac{1 - \sqrt{1 - 2f}}{2f}$$
$$= 0.582$$

We can see from Figure 7 that the value of C at the limit line will be about 0.8 for $C_i = 0.58$, that is $A_{2'}/A_{*2}$ will be about 1.25 and $(A/A_*)_{2'}$ rather less than this value.

We now guess a value for $M_{2'}$ at choking and use Equations (8), (7) and (2) to determine whether this value fits.

Guess $M_{2'} = 1.52$, $\left(\frac{P_t}{P_s}\right)_{2'} = 3.7792$, $\left(\frac{A}{A_*}\right)_{2'} = 1.1899$

From Equation (8), $C = 0.792$

When $M_{2'} = 1.52$, $M_3 = 0.6941$ (from shock tables)

$$\left(\frac{P_t}{P_s}\right)_3 = 1.3799, \quad \left(\frac{A}{A_*}\right)_3 = 1.0987, \quad \left(\frac{\rho_t}{\rho_s}\right)_3 = 1.2586$$

With $f = 0.2407$ and these values inserted in Equation (7) we get

$$\frac{P_{t_3}}{P_{t_1}} = 0.8843$$

From Equation (2), with $(A/A_*)_2 = 1$ we get

$$C = \frac{0.8843}{1.0987}$$

$$= 0.8049$$

Since the two values of C do not match we choose another value for $M_{2'}$, say $M_{2'} = 1.5$. The result now is that $C = 0.8071$ and 0.8077 from which we expect the value of C at the limit to be 0.808. Therefore, the value of W/W_* at the limit is 0.808.

APPENDIX III

Analysis of intake performance with bleed flow

Referring to Figure 11, the total pressure at station 4 is taken to be the mass-weighted sum of the total pressures of the two flows at the point where they are both wholly within the intake duct.

$$W_4 \, P_{t_4} = W_1 \, P_{t_4'} + W_5 \, P_{t_5'}$$

It is assumed that $P_{t_4'}$ is equal to the total pressure which would occur at station 4 with the bleed slot blanked and the same flow W_1 entering the intake inlet. In Table II the resultant total pressure $P_{t_5'}/P_{t_1}$ of the bleed flow has been estimated from the experimental results, using flow proportions estimated from the cowl lip static pressure measurements. In the second part of the table, the static pressure required in the bleed slot passage if the estimated flow rate W_5 is to enter is compared with the observed static pressure at station 4'.

The loss $(P_{t_1} - P_{t_5'})$ is also expressed as a proportion of the bleed air dynamic head $(P_{t_1} - P_{s_4})$.

In Table III an estimate of the intake pressure recovery at various slot openings has been made wholly from the no-bleed pressure recovery characteristics, assuming only that $P_{s_5} = P_{s_4'}$ and $(P_{t_1} - P_{t_5'}) = 0.15 \, (P_{t_1} - P_{s_4})$. The differences between the pressure recoveries calculated in this way and the experimentally observed values are not greater than the probable experimental errors.

FIG. I.

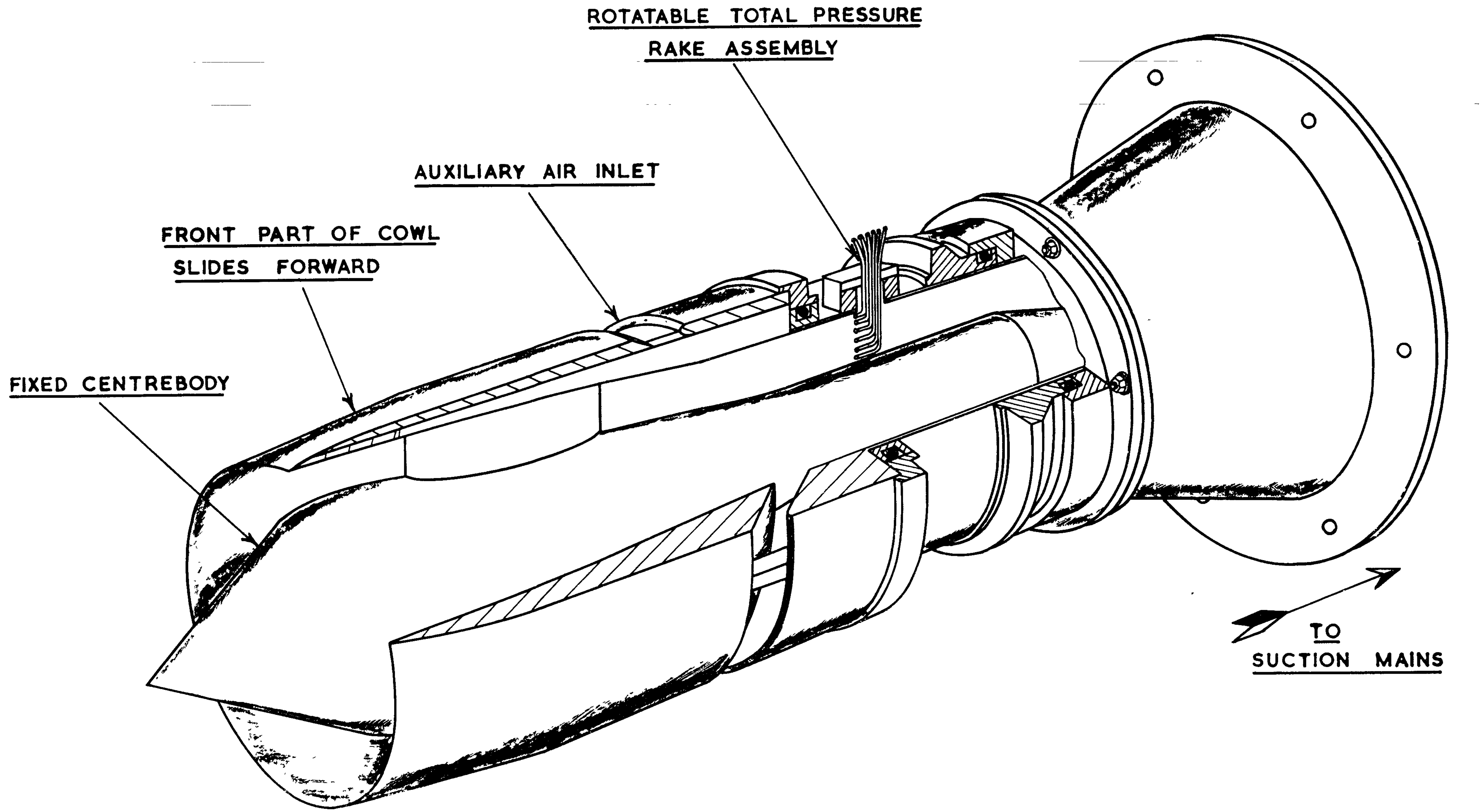

GENERAL ARRANGEMENT OF MODEL INTAKE

FIG. 2

DISTANCE FROM LIP - IN	3·5	4·0	4·5	5·0	5·5	6·0	6·5	7·0	7·5
BLOCKAGE AREA - IN²	0	1·365	2·652	2·859	3·015	3·159	3·258	1·902	.0

BLOCKAGE OF ANNULUS CROSS-SECTIONAL AREA DUE TO SUPPORT WEBS.

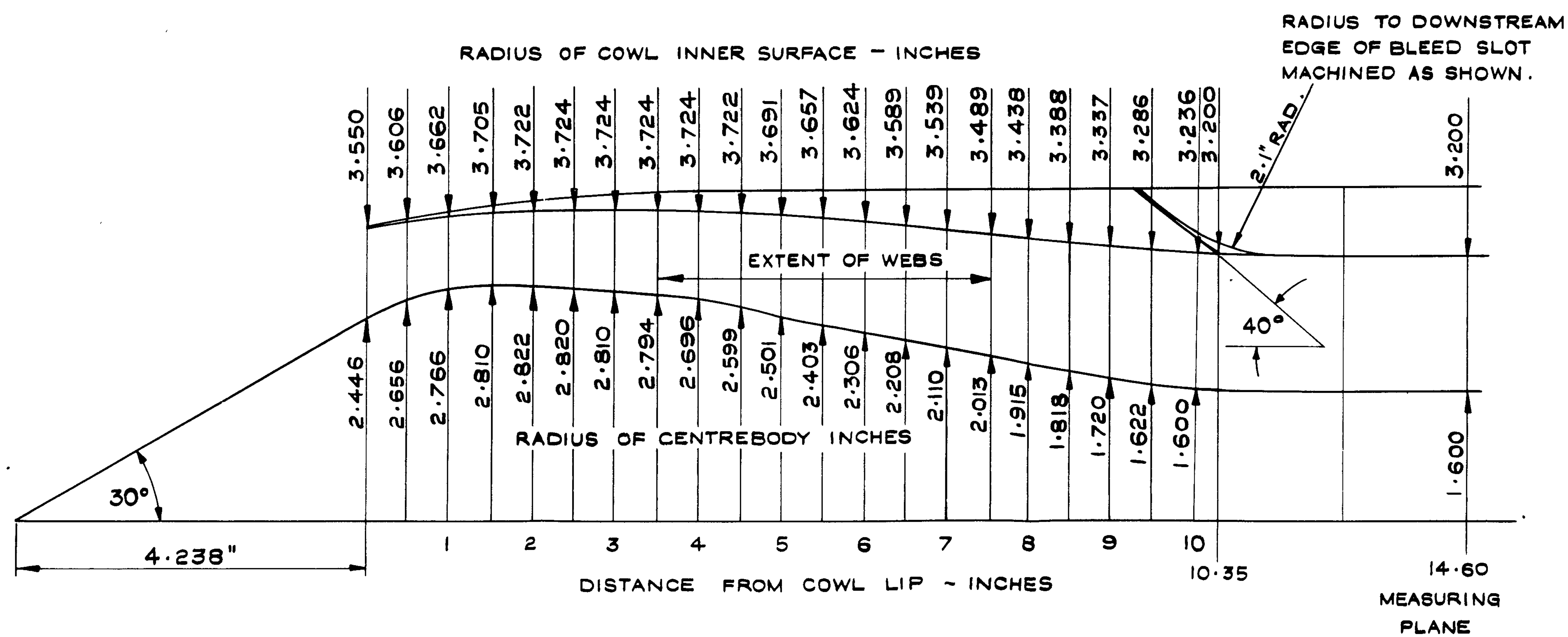

INTAKE ANNULUS CO-ORDINATES.

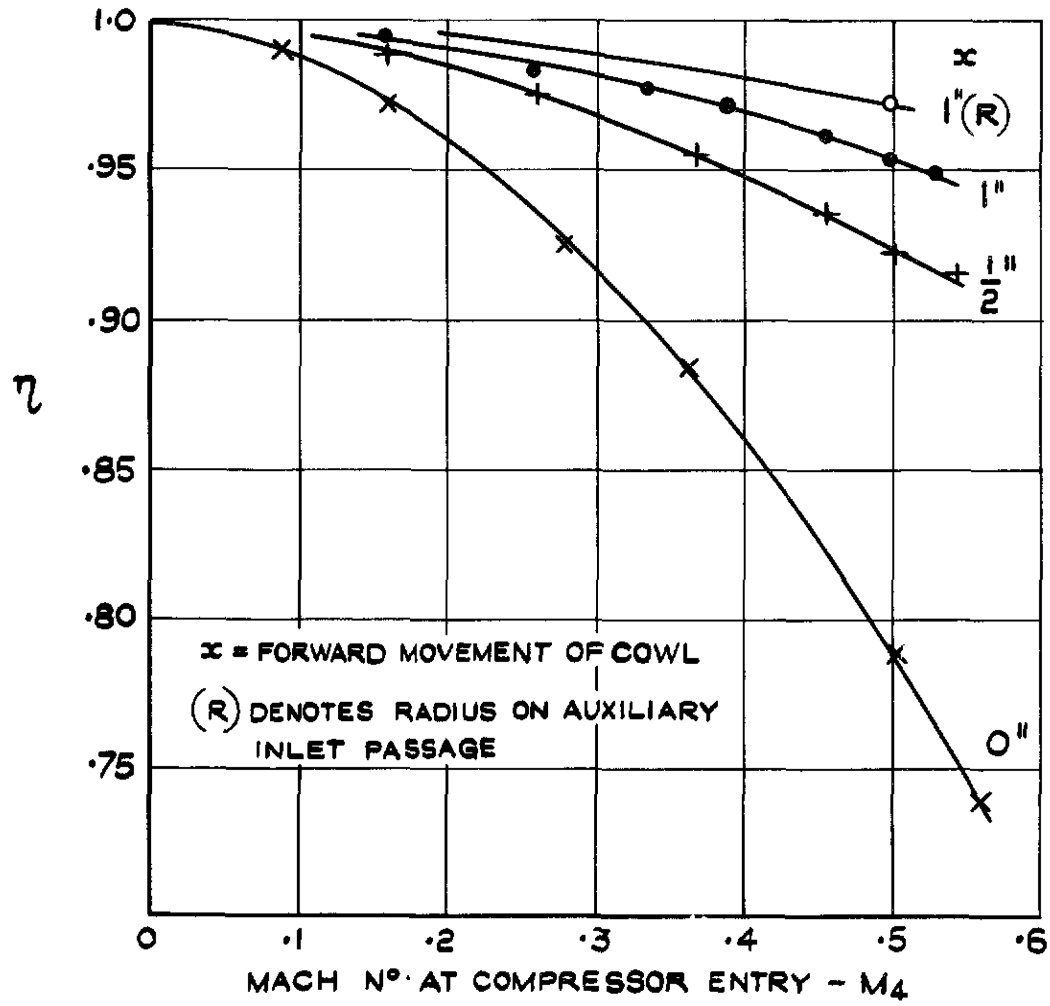

FIG. 3. INTAKE PRESSURE RECOVERY CHARACTERISTICS.

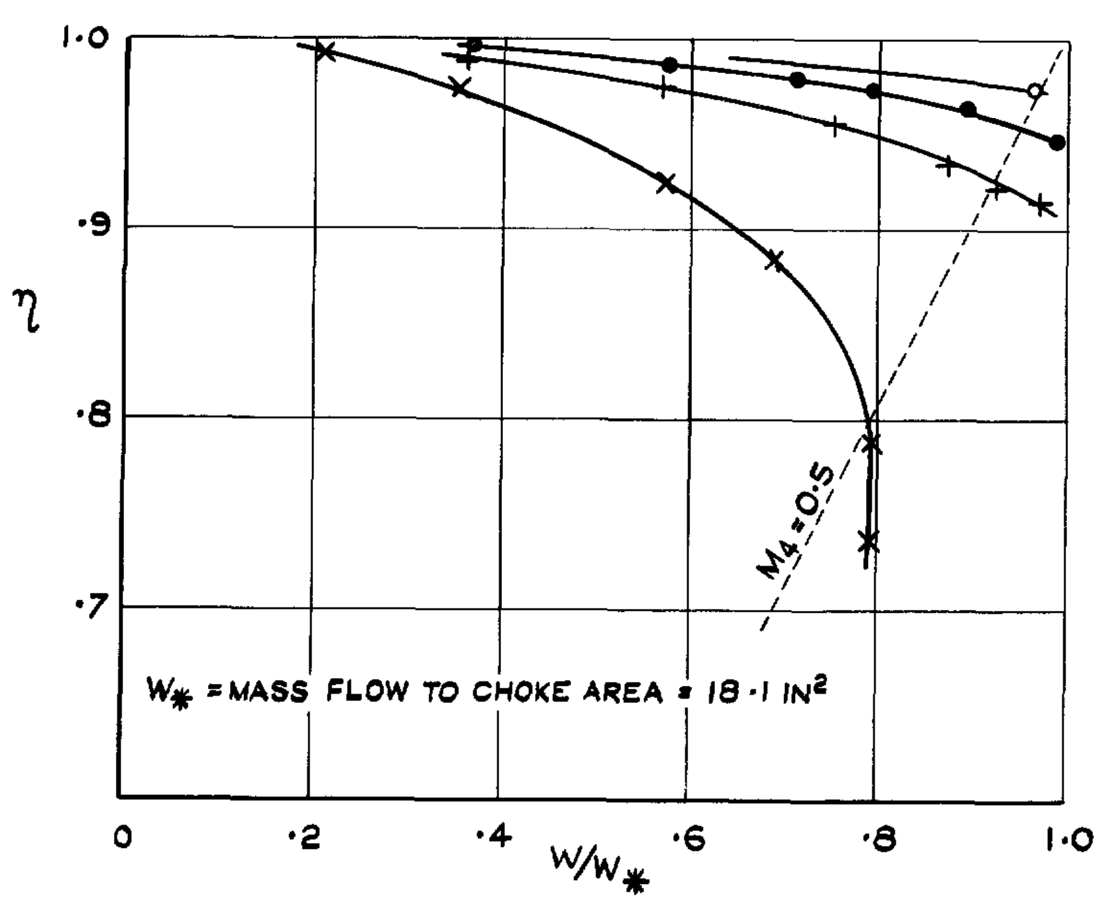

FIG. 4. INTAKE PRESSURE RECOVERY vs FLOW RATIO $\frac{W}{W_*}$

FIG. 5

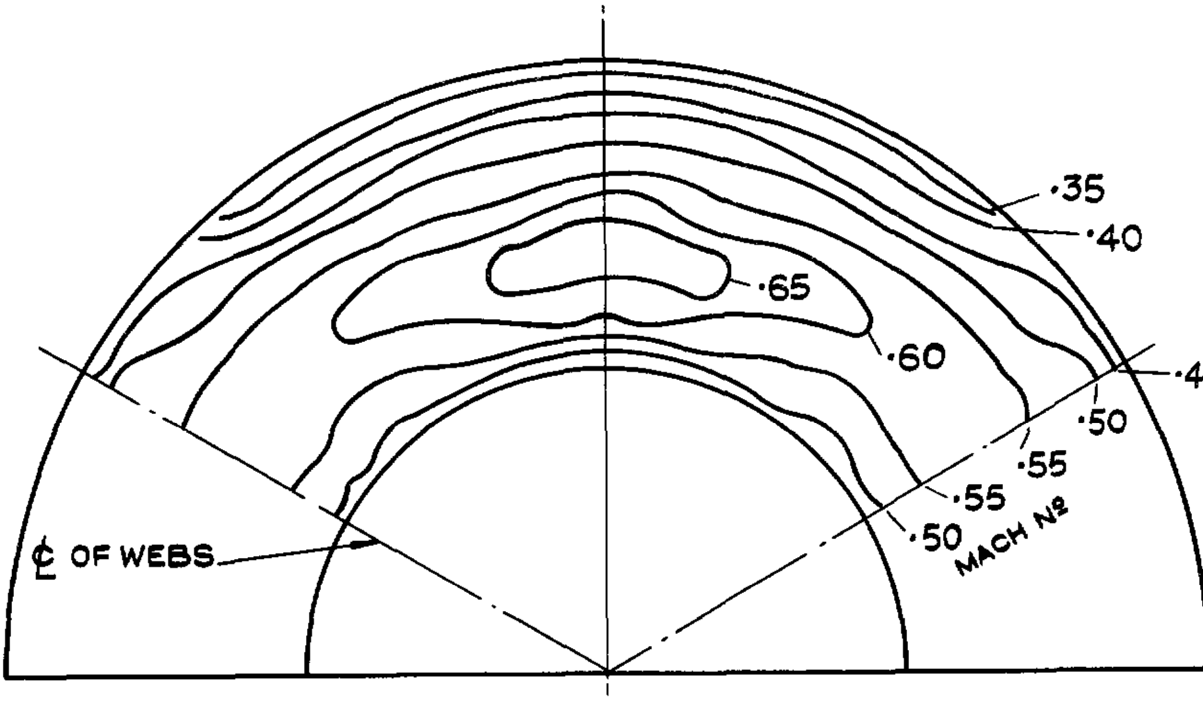

MEAN MACH Nº = 0·502 MAX. MACH Nº = 0·67

PRESSURE RECOVERY = 0·788 VELOCITY RATIO $\frac{V\,MAX.}{V\,MEAN}$ = 1·31

VELOCITY DISTRIBUTION WITH BLEED SLOT SHUT.

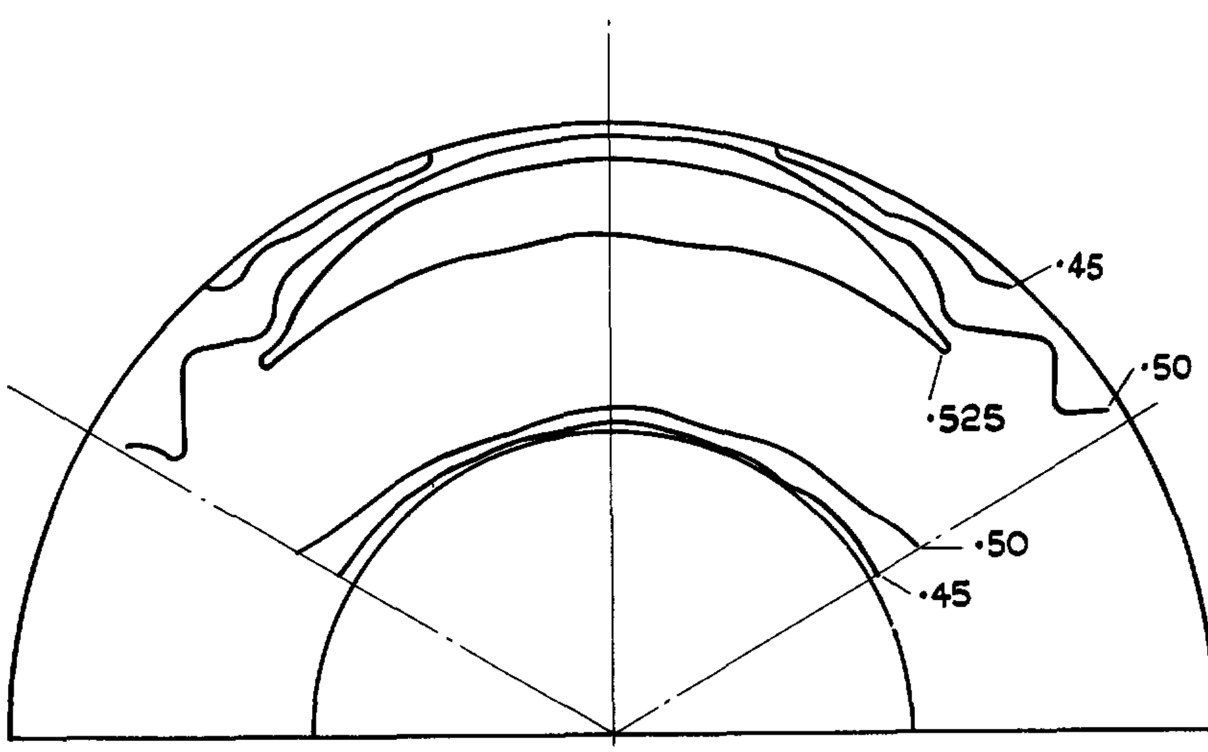

MEAN MACH Nº = 0·498 MAX. MACH Nº = 0·548

PRESSURE RECOVERY = 0·972 VELOCITY RATIO $\frac{V\,MAX}{V\,MEAN}$ = 1·095

VELOCITY DISTRIBUTION WITH BLEED SLOT 1" OPEN.

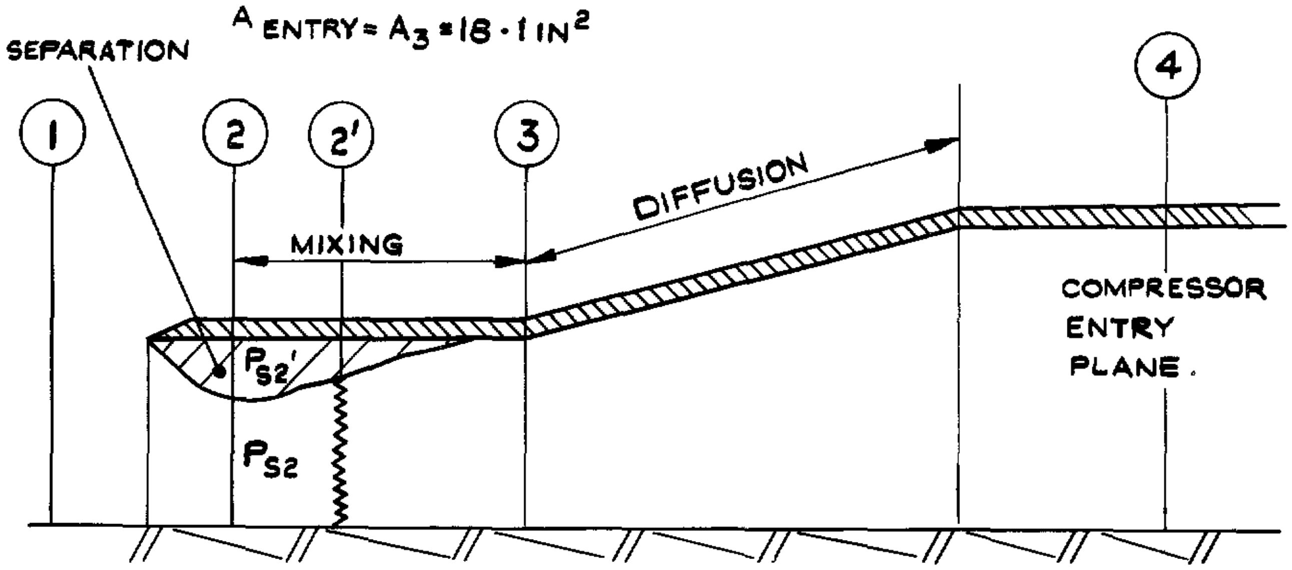

FIG. 6. DIAGRAMMATIC ARRANGEMENT OF ASSUMED SIMPLIFIED INTAKE DUCT.

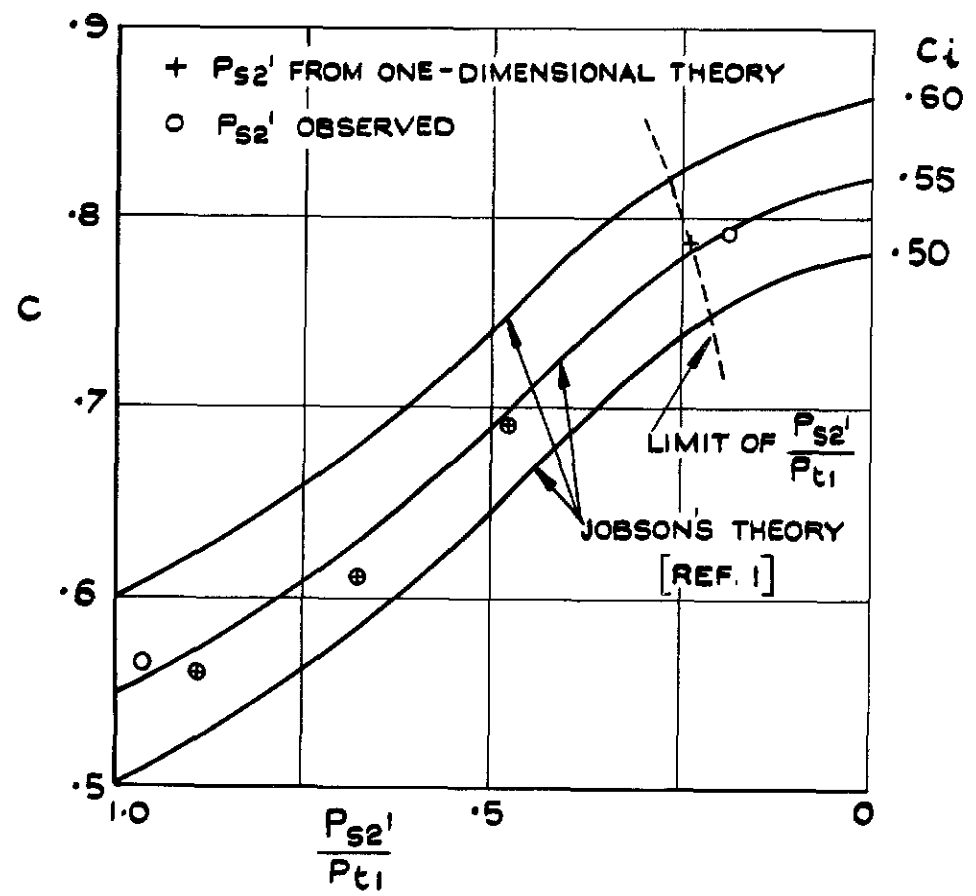

FIG. 7. CONTRACTION COEFFICIENT ESTIMATED BY SIMPLIFIED ONE DIMENSIONAL ANALYSIS.

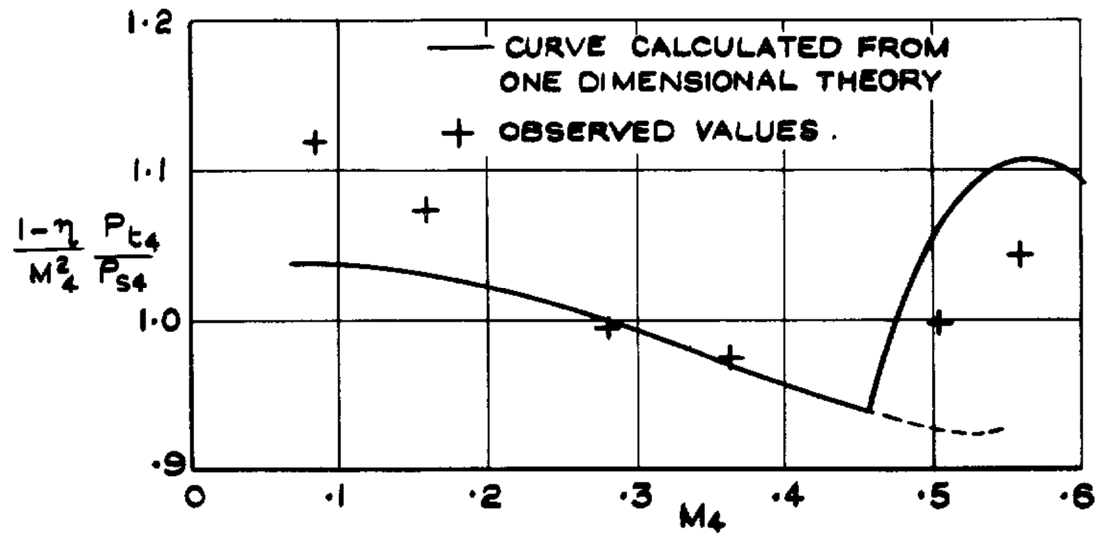

FIG. 8. COMPARISON OF CALCULATED AND OBSERVED PRESSURE RECOVERIES.

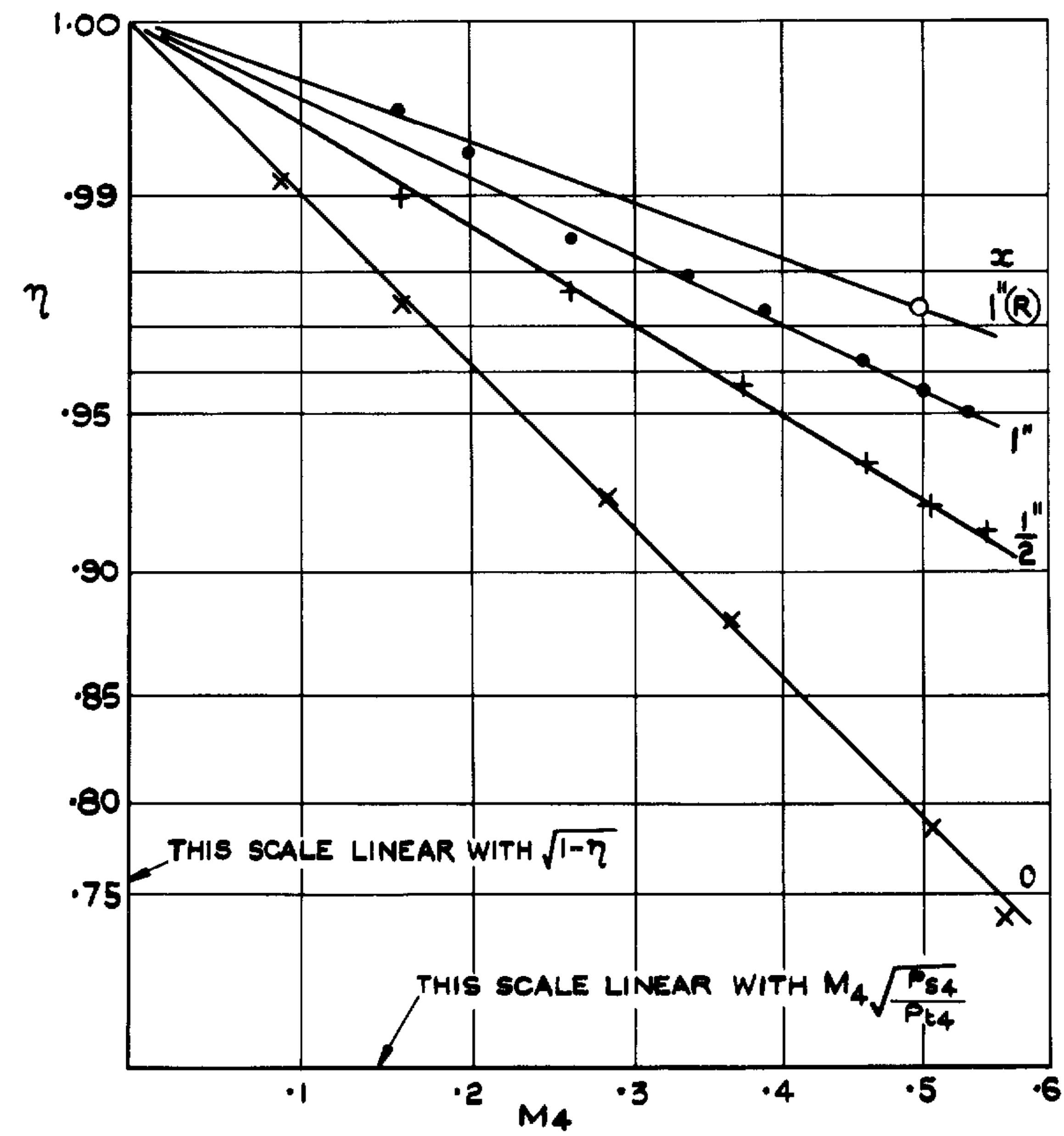

FIG. 9. INTAKE CHARACTERISTICS TO SCALES $\sqrt{1-\eta}$ vs $M\sqrt{\frac{P_s}{P_t}}$

FIG. 10.

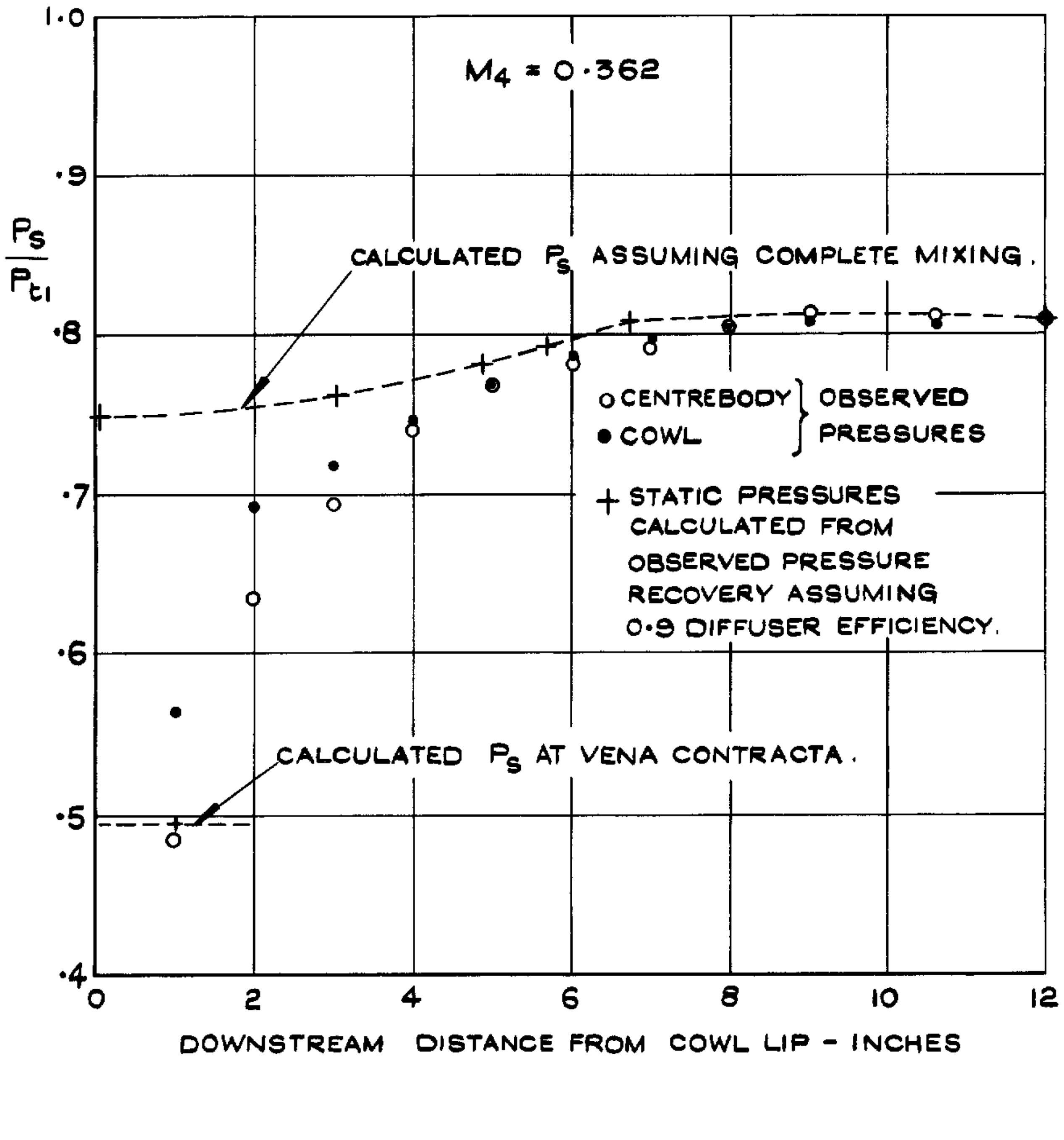

OBSERVED INTAKE DUCT STATIC PRESSURES COMPARED WITH ONE DIMENSIONAL ESTIMATE.

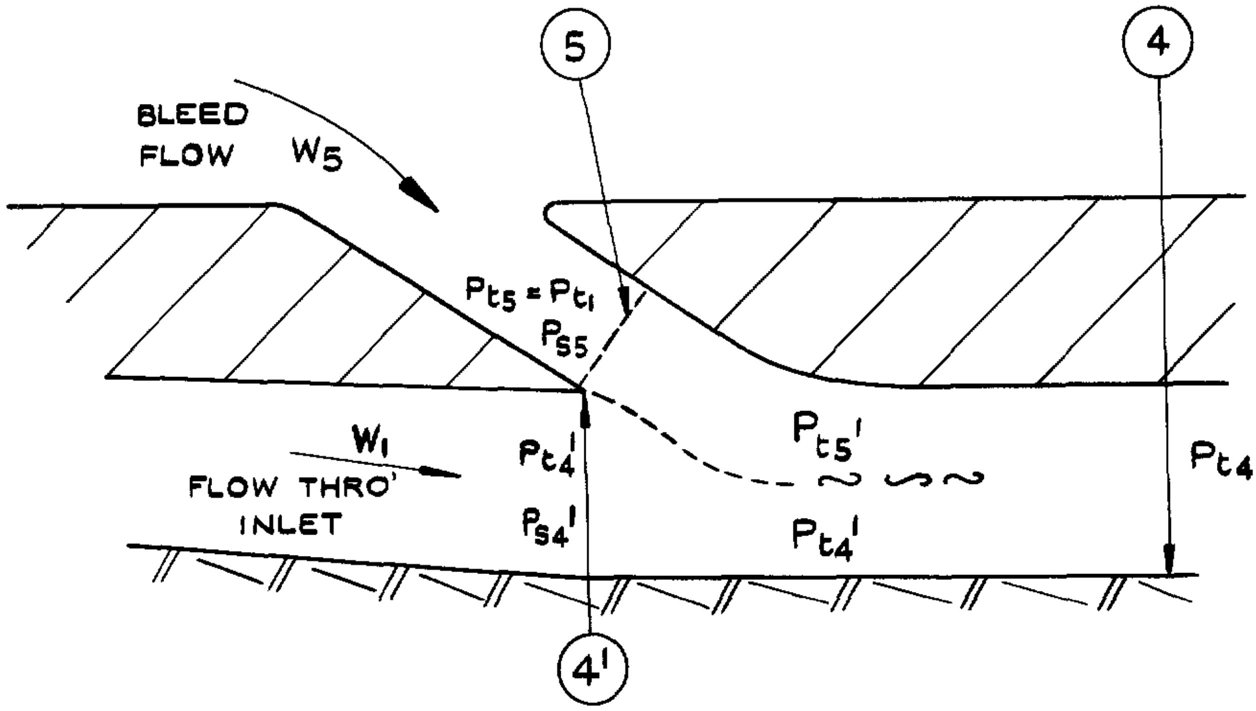

FIG. 11. DIAGRAMMATIC ARRANGEMENT OF FLOW THROUGH BLEED SLOT.

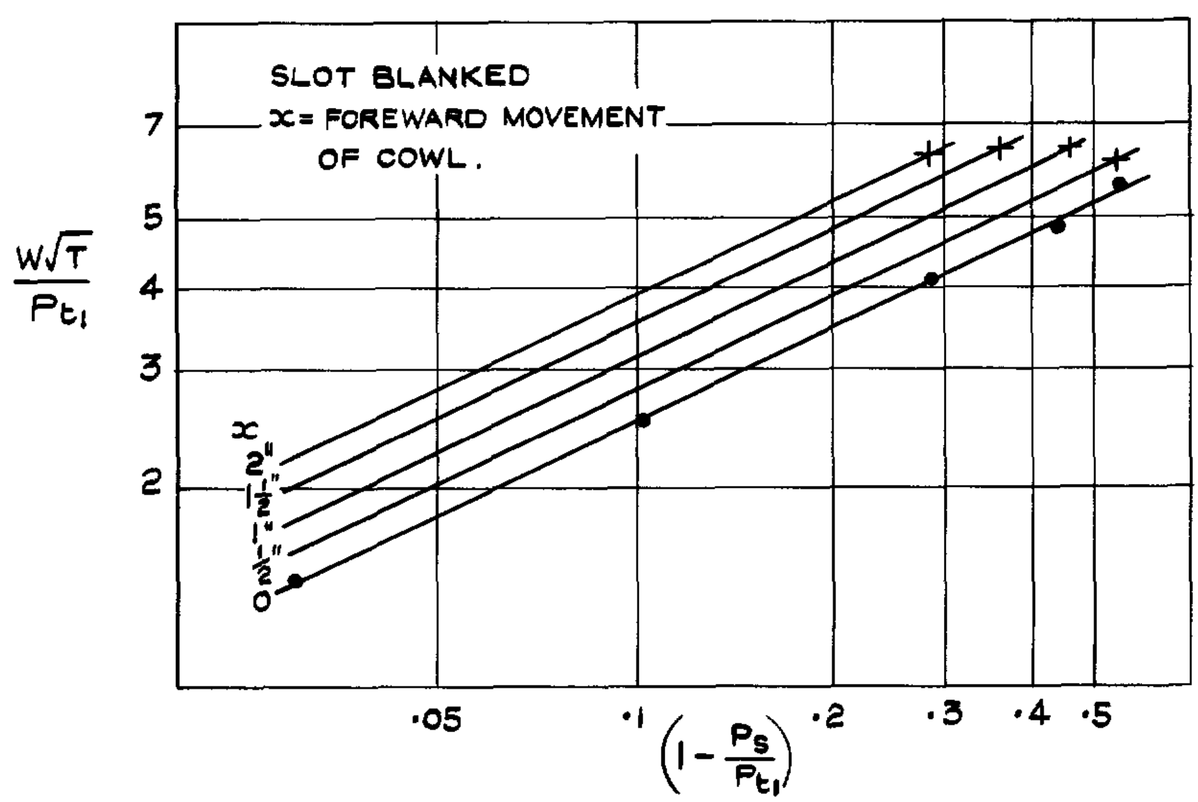

FIG. 12. RELATION BETWEEN FLOW INTO INTAKE AND STATIC PRESSURE INSIDE COWL LIP.

DS 80942/1/Wt. 60 K. 4 9/60 R & CL

C.P. No. 515
(21,032)
A R C Technical Report

Printed and published by
HER MAJESTY'S STATIONERY OFFICE

To be purchased from
York House, Kingsway, London w.c.2
423 Oxford Street, London w.1
13A Castle Street, Edinburgh 2
109 St. Mary Street, Cardiff
39 King Street, Manchester 2
50 Fairfax Street, Bristol 1
2 Edmund Street, Birmingham 3
80 Chichester Street, Belfast 1
or through any bookseller

Printed in England

S.O. Code No. 23-9012-15

C.P. No. 515